Neurogenic flare response following image-guided focused ultrasound in the mouse peripheral nervous system *in vivo*

Min Gon Kim[1], Hermes A S Kamimura[1], and Elisa E Konofagou[1,2]

[1]Department of Biomedical Engineering, Columbia University, New York, NY, USA

[2]Department of Radiology, Columbia University, New York, NY, USA

*Corresponding Author: Elisa E Konofagou, Ph.D., ek2191@columbia.edu; +1-212-342-0863

ABSTRACT

Focused ultrasound (FUS) has been used to noninvasively elicit or inhibit motor neuronal activity in the mouse peripheral nervous system in vivo. However, less is known about whether FUS elicits immune system responses associated with peripheral sensory neuronal activity. In this study, we demonstrate that non-invasive ultrasound image-guided FUS can elicit the neurogenic axon reflex of peripheral nerves in the mouse sciatic nerve. The local vasodilation in the plantar view of the hind paw detected by a high-resolution laser Doppler imager indicated neurogenic flare responses following FUS stimulation. The effects of FUS were compared with control groups, where a distinct pattern of blood flow changes was only observed in FUS-elicited neurogenic flare responses. The findings indicate that image-guided FUS elicits local axon reflexes in vivo with a high degree of specificity and penetration depth.

Keywords:

Image-guided focused ultrasound; immune system function; mouse sciatic nerve; neurogenetic axon reflex; sensory neural activity.

Introduction

Implementing new scientific findings by altering the activity of populations of neurons in clinical practice has been an ongoing mission in basic and clinical neuroscience (Moe and Post 1962; Sheffler and Chae 2007; George et al. 2010; Fontaine et al. 2018). The functional assessment of the peripheral nervous system has demonstrated the interaction between the peripheral nervous and immune systems (Chiu et al. 2012; Talbot et al. 2015) and paved the way for the development of diagnostic and treatment methods for numerous disorders (Skaper et al. 2018; Anandagoda el al. 2019). For example, prior studies have provided evidence that the activity of peripheral sensory neurons directly acts on the vasculature (Magerl et al. 1987; Lin et al. 1999; Lin et al. 2003) and elicits innate and adaptive immune cells (Mikami et al. 2011; Rochlitzer et al. 2011; Chiu et al. 2012) through the neurogenic axon reflex mediated by the release of the neuropeptides in the peripheral nervous system. In addition, researchers have demonstrated the feasibility of a diagnostic tool based on the measurement of neurogenetic inflammation such as complex regional pain syndrome patients along with a significant increase in axon reflex vasodilation (Weber et al. 2000) and small fiber neuropathy patients closely associated with diabetes or autoimmune diseases (Hovaguimian et al. 2011) along with a significant decrease in axon reflex flares (Kramer et al. 2004) compared to the amount of axon reflex flares in control groups. Therefore, a range of neuromodulation techniques has been developed to better interpret the roles of peripheral neurons and regulate peripheral immune system functions by inducing vasculature (flare) as well as activating immune cells through the release of inflammatory mediators (Chiu et al. 2012). Chemical stimulation has been demonstrated to evoke acute neurogenic flare responses (Jancsó et al. 1967; Jancsó et al. 1968; Lin et al. 2003) by activating the efferent activity of sensory neurons (Lin et al. 1999). However, the clinical use of this method may be limited due to a low degree of specificity and penetration depth as well as undesirable side effects, such as burning or stinging of the skin. Transcutaneous electrical stimulation has

been proposed as an alternative approach to induce axon reflexes by delivering an electrical current into a targeted region via electrodes placed on the surface of the skin (Magerl et al. 1987; Weidner et al. 1999). However, despite its effectiveness, this method suffers from the inability to target deep regions, and it affects a broad area rather than a specific target region due to low spatial precision. In addition, a strong electrical intensity is needed to elicit afferent fibers of nociceptors, including myelinated Aδ and unmyelinated C fibers, causing unpleasant sensations (Magerl et al. 1987; Sauerstein et al. 2000). Therefore, there remains a need for the development of new neuromodulation techniques with high spatial precision and the ability to target deep regions.

Focused ultrasound (FUS) is a promising method capable of noninvasively modulating peripheral neuronal activity in specific regions with a high degree of specificity and penetration depth. Prior *in vitro* and *in vivo* studies have demonstrated the feasibility of FUS for modulating peripheral neuronal activity and understanding the functions of the peripheral nervous system. For example, Mihran et al. presented both the enhancement and suppression of electrically evoked compound action potentials through the mechanical effect in the frog sciatic nerve *in vitro* (Mihran et al. 1990). Moreover, Tsui et al. demonstrated the enhancement and suppression of electrically activated compound action potentials in the frog sciatic nerve *in vitro* along with FUS-mediated temperature elevation of 3ºC and 6–10ºC, respectively (Tsui et al. 2005). Colucci et al. showed a temporary nerve block by a temperature increase of approximately 17–23°C in the frog sciatic nerve *in vitro* (Colucci et al. 2009). In addition, Wright et al. reported evoked de novo action potentials via the mechanical effect in the crab leg nerve *ex vivo* (Wright et al. 2017). In this regard, these findings contributed to elucidating potential mechanisms in well-established *in vitro* and *ex vivo* setups. Nonetheless, these studies have primarily investigated limited interactions between FUS and the inherent complexity of neuronal activity in the peripheral nervous system.

Furthermore, *in vivo* animal studies have been conducted to understand better the effect of FUS on peripheral neural activity, which is a crucial step toward improvements for the

technique's clinical translation. Previous studies have indicated that temporary or permanent nerve blocks can suppress motor neural activity in the sciatic nerve of the rabbit and rat (Foley et al. 2004; Foley et al. 2007; Foley et al. 2008), activated by the mechanical effect in the mouse sciatic nerve (Downs et al. 2018), and activated or inhibited as a function of transient temperature elevation in the mouse sciatic nerve (Kim et al. 2020). In addition to modulating motor neuronal activity, studies have shown the use of FUS to modulating anti-inflammatory or metabolic pathways by stimulating the spleen or liver, respectively (Cotero et al. 2019) and identifying the neural-immune interaction by targeting the spleen (Zachs et al. 2019). However, it has not been shown whether FUS can directly activate peripheral afferents causing local axon reflexes, leading to a robust flare response in the skin.

In this study, we demonstrate the capability of image-guided FUS in eliciting the neurogenic axon reflex of peripheral nerves *in vivo*. We hypothesized that FUS (< spatial peak pulse average intensity (I_{SPPA}) of 190 W/cm^2 and < mechanical index (MI) of 1.9) can evoke the neurogenic axon reflex in the mouse sciatic nerve *in vivo* without affecting the motor neuronal response - a known drawback of transcutaneous electrical stimulation (Magerl et al. 1987; Sauerstein et al. 2000). We used a high-resolution Doppler imager to investigate local vasodilation in the plantar view of the hind paw following the FUS stimulation of distal portions of the sciatic nerve and compared blood flow measurements with control groups to determine whether FUS at the distal sciatic nerve elicits the neurogenic axon reflex.

Materials and Methods

In vivo animal preparation

All animal procedures were approved by the Institutional Animal Care and Use Committee of Columbia University and Animal Care and Use Review Office. Wild type mice C57BL/6J

weighing between 22 g to 26 g were anesthetized with isoflurane concentrations of 4% for induction and 1.75% to 2% for maintenance throughout the experiment. The targeted hind limb was shaved by depilatory cream for hair removal at least 3 days before the experiments. Normal body temperature was maintained throughout the experiments using a heating pad. The depth of anesthesia was frequently monitored through the pedal reflex.

Experimental setup and blood flow measurement

The experimental setup consisted of a FUS transducer with an ultrasound imaging transducer, a three-dimensional (3D) positioning system, a high-resolution laser Doppler imager, and blood flow recording and analysis equipment, as presented in Figure 1(a). The imaging transducer with the frequency spectrum of 5-12 MHz (P12-5, ATL/Philips, Bothell, WA, USA) connected to a Vantage 128 research platform (Verasonics; Kirkland, WA, USA) was co-aligned with a 3.1 MHz single element FUS transducer (H-108, Sonic Concepts, Inc., Bothell, WA, USA). A function generator connected to a 50-dB power amplifier and matching network were used to drive the FUS transducer following parameters, including peak-to-peak voltage (V_{pp}), pulse duration (PD), pulse repetition frequency (PRF), and total sonication time. A 3D linear translation/rotation stage (BiSlide MN10-0100-M02-21, Velmex, Bloomfield, NY, USA) controlled by a customized MATLAB program (MathWorks Inc., Natick, MA, USA) was used to precisely place the image-guided FUS transducer at the desired location.

FUS with a peak positive/negative pressure of 1.96/1.95 MPa, PD of 1 ms, PRF of 100 Hz, and total sonication time of 10 min was applied to the distal sciatic nerve for eliciting an acute flare reaction (n=8 hindlimbs of mice) after precisely finding and locating the targeted distal sciatic nerve (Kim et al. 2020). The axial and lateral focal dimensions measured by a hydrophone (HGL-0200, Onda Corp., Sunnyvale, CA, USA) were 4.16 mm and 0.42 mm, respectively, based on the full width at half maximum (FWHM, −6 dB pressure) of the pressure field.

A high-resolution laser Doppler imager with the measurement software program (moorLDI2-HIR System, Moor Instruments Inc., Wilmington, DE, USA) was used to measure the blood flow change at the plantar view of the hind paw along with FUS at the distal sciatic nerve, which was extracted the time-based blood flow change using an analysis software program and further analyzed in terms of vasodilation area and intensity using a customized algorithm written in MATLAB. Figure 1(b) presents the baseline blood flow recorded for 15 min before FUS stimulation, and the blood flow changes continuously measured during and after FUS stimulation for 45 min. According to the sciatic nerve innervation's anatomy in the hind paw (Zhi et al. 2017), the digits 3, 4, and 5 of the hind paw innervated to the sural and tibial nerves are the branches of the sciatic nerve. The recorded time-resolved blood flow changes of paw digits 3, 4, and 5 in the hind paw was analyzed in terms of time-to-peak (time elapsed from the onset of FUS until peak increase in blood flow), response latency (time elapsed from the onset of FUS until a threefold increase in the standard deviation of individual baseline blood flow obtained by each experiment), area under the curve (the area from the onset of FUS to the end of the recording), and peak increase in blood flow (maximum blood flow from the onset of FUS until the end of recording). The values of the peak increase in blood flow and area under the curve were normalized to each experiment's individual baseline value prior to FUS. Response latency was detected through thresholding the blood flow value greater than three times the standard deviation from the individual baseline value obtained by each experiment.

Control experiments

Control experiments were performed to rule out other potential sources of electric charges affecting blood flow measurements. The acute flare reaction from FUS was compared with those obtained from three control experiments: (1) deactivating the FUS driving system without changing the rest of the experimental setup (n=7 hindlimbs of mice), (2) applying 20 dB attenuated FUS with different driving conditions (driving the transducer outside its frequency bandwidth

(center frequency of 3.1 Hz with PRF of 0.1 Hz)) without modifying the rest of the experimental setup (n=6 hindlimbs of mice) to investigate the effect of potential sources of electromagnetic noise on the blood flow measurement while activating FUS driving system, and (3) applying off-target FUS at 2.5 mm away from the nerve with the same experimental setup (n=6 hindlimbs of mice). In addition, FUS with a total sonication time of 3 min (n=2 hindlimbs of mice) and electrical stimulation (S48 stimulator, Grass Technologies, West Warwick, RI) with custom-built electrical stimulation wire were separately conducted. For electrical stimulation, we used 50% of the electrical stimulation voltage (2–3V), where 100% of the electrical stimulation voltage (4–6V) was capable of evoking muscle activation in each experiment (n=2 hindlimbs of mice) to compare FUS-induced induced flare response.

Data analysis

The measured values were expressed as mean ± standard error of the mean. Statistical analysis was conducted to compare unmatched groups with individual variances through the Student's t-test and multivariable ANOVA using commercial statistics software (Prism, GraphPad Software, San Diego, CA, USA). Statistical significance was denoted as $p < 0.05$ * and $p < 0.01$ **.

Results

FUS-induced axon reflex vasodilation

Figure 2 and Supplementary Figures S1 show the representative axon reflex vasodilation induced by FUS stimulation along with results obtained from two negative control groups. In Figure 2(a), FUS induced a distinct blood flow pattern: increased blood flow during FUS, rapidly decreased blood flow, and steadily increased blood flow after FUS stimulation. However, the

corresponding values from the two negative control groups remained mostly at a constant baseline blood flow. The effect of FUS on the recorded blood flow was then quantified in terms of time-to-peak, response latency, area under the curve, and peak increase in blood flow as shown in Figure 2(b)-(e). For the time-to-peak (Figure 2(b)), the values from FUS were not significantly different from the values of the two negative control groups. The groups were divided as follows: n=8 for FUS stimulation group, n=7 for negative control group without activating FUS driving system (p-value=0.506), n=6 for the negative control group with 20 dB attenuated FUS with a different center frequency of 3.1 Hz and PRF of 0.1 Hz without any other changes in the experimental setup (p-value=0.086). However, as shown in Figure 2(c)-(e), the average response latency was found to decrease by 12.3–16.7 min, and FUS resulted in an increased average normalized area under the curve and average peak increase in blood flow by 12.3–13.1% and 50.6–50.8%, respectively, which were significantly different from the values of the two negative control groups. FUS stimulation at the distal sciatic nerve resulted in a noticeable increase in the blood flow responses, which in turn reduced the response latency (Figure 2(c)) and increased the area under the curve (Figure 2(d) and peak increase (Figure 2(e) during and after FUS stimulation.

Evaluation of axon reflex vasodilation in response to sciatic nerve stimulation

We compared axon reflex vasodilation resulting from the FUS at sciatic nerve (on-target) and FUS at 2.5 mm away from the nerve (off-target). Figure 3 and Supplementary Figures S1 indicate the blood flow change between FUS stimulation at the focus (i.e., effects of sciatic nerve stimulation) and 2.5 mm from the focus (i.e., off-target effects of sciatic nerve stimulation). The increased blood flow during FUS stimulation at the sciatic nerve or off-target region primarily resulted from the FUS-induced thermal effect (9.8 ± 1.0ºC from the temperature at pre-FUS stimulation, 30.3 ± 0.2ºC, n=3) based on our temperature estimation procedure (Kamimura et al. 2020; Kim et al. 2020). However, compared to off-target effects, a distinct blood flow pattern was observed following FUS stimulation, which may be associated with neurogenic inflammation. As

shown in Figure 3(b) and (d), the average time-to-peak was found to increase from 16.8 ± 16.9 min (off-target) to 36.3 ± 11.1 min (on-target), and the average normalized area under the curve was increased from 3.5 ± 4.8 (off-target) to 15.5 ± 13.9 (on-target), which was significantly different (p-value < 0.05, n=8 for FUS stimulation at sciatic nerve, n=6 for FUS stimulation at 2.5 mm away from the focus). However, response latency (Figure 3(c)) and peak increase in blood flow (Figure 3(e)) were not significantly different from those of the off-target results (p-value=0.102 and 0.108, respectively). Furthermore, a simulation of the spatial FUS-induced heating in the mouse leg indicates that the temperature effects are highly localized within the lateral focal dimension of 0. 42 mm compared to calculated distance between estimated distal sciatic nerve and muscle for EMG recording (4 mm) as well as calculated distance between muscle region and the plantar view of the hind paw (15.7 mm) (Supplementary Figure S2). This indicates that a heating diffusion from the sonication site to the plantar view of the hind paw is not expected. Therefore, the blood flow changes were associated with a neurogenic flare response.

Discussion

This study presented the neurogenic flare response in the mouse peripheral nervous system *in vivo* using image-guided FUS (I_{SPPA} of 71 W/cm^2 and MI of 1.1). We examined the effect of FUS on the distal sciatic nerve along with time-based blood flow change at the plantar view of the hind paw after precisely and noninvasively locating and targeting the distal sciatic nerve. Control experiments determined that the FUS-induced neurogenic axon reflex produced a distinct pattern of blood flow elevation.

In previous studies, chemical or transcutaneous electrical stimulation has been used to elicit neurogenic inflammation where activation of the afferent fibers of nociceptors including myelinated Aδ and unmyelinated C fibers results in vasodilation and/or protein extravasation.

According to the results shown in Figure 4, electrical stimulation with subthreshold intensity was not enough to elicit axon reflex vasodilation, which was consistent with previously published studies (Magerl et al. 1987; Sauerstein et al. 2000). However, FUS (I_{SPPA} of 71 W/cm^2 and MI of 1.1) with temperature elevation up to 40.1 ºC for 10 min can evoke the neurogenic axon reflex in the mouse sciatic nerve *in vivo* without activating the motor neuronal response that was measured in electromyography (EMG) signal at the gastrocnemius muscle. This is significant because it demonstrates the feasibility of FUS-induced orderly activation of neuronal activity in the peripheral nervous system *in vivo* by adjusting the FUS intensity level (Young and Henneman 1961; Kim et al. 2020). In addition, FUS with a total sonication time of 3 min induced a blood flow change pattern similar to that from FUS with a total sonication time of 10 min, as shown in Figure 4: a gradual increase in blood flow during FUS, rapid decrease, and steady increase in blood flow after FUS. The effect of FUS with various parameters will be investigated in future studies to understand the FUS-induced neurogenic flare response better.

We demonstrated the feasibility of FUS for direct activating of the peripheral neuronal activity underlying either sensory afferent or motor efferent fibers by adjusting FUS parameters at the same targeted nerve region. Based on our previous study (Kim et al. 2020), we applied short/high-intensity FUS (I_{SPPA} of 6610 W/cm^2) to activate motor neurons innervating muscle activity for the targeting procedure and long/low-intensity FUS (I_{SPPA} of 71 W/cm^2) to activate sensory neurons for the neurogenic inflammation. The exact mechanism remains unclear. However, the vasodilation observed in this study indicates that FUS activates peripheral afferents of peptidergic nociceptors, including myelinated Aδ and/or unmyelinated C fibers and, consequently, the peripheral release of neuropeptides. Thus, to better understand the mechanism, future studies remain necessary to determine (1) the functional roles of particular afferent fiber types by depleting their neuropeptides and (2) the functions of neurotransmitter receptors by using antagonists (Sluka et al. 1995; Lin et al. 2003).

Here, as an extension of controlling motor neuron activity, we monitored local axon reflexes induced by FUS stimulation more than 4 mm away from the recording area using a quantitative readout of blood flow in the mouse peripheral nervous system *in vivo*. The neurogenic axon reflex was observed with FUS stimulation at the sciatic nerve compared to negative control groups with off-target effects of sciatic nerve stimulation. Based on the results in this paper, the FUS-induced axon reflexes can be applied to determining small fiber neuropathy in diabetes as a diagnostic tool (Kramer et al. 2004). In addition, once a deeper understanding of the functions of particular afferent fiber types along with neurotransmitter receptors can be established, a new FUS-based therapeutic strategy may be formulated to regulate immune system functions and ultimately provide clinical medicine for the treatment of immune diseases (Chiu et al. 2012).

Conclusion

The neurogenic flare response following image-guided FUS was demonstrated in the mouse peripheral nervous system *in vivo*. Building on the previously established targeting procedures for precisely and noninvasively finding the targeted sciatic nerve *in vivo*, we used a high-resolution laser Doppler imager in the image-guided FUS system to quantitatively assess the local vasodilation in the plantar view of the hind paw as evidence of the elicited neurogenic flare response. We identified the FUS-induced neurogenic flare response by comparing blood flow changes with those of control groups. These experimental findings indicate that image-guided FUS could be applied for reliably detecting small fiber impairment in diabetic neuropathy as a diagnostic method or regulating immune system functions by selectively eliciting peripheral sensory neuronal activity.

Acknowledgments

This study was supported in part by the Defense Advanced Research Projects Agency (DARPA) under Grant No. HR0011-15-2-0054 and the National Institutes of Health under Award No. R01EB027576.

The authors thank Dr. Ellen Lumpkin, Dr. Chi-Kun Tong, Dr. Danny Mauricio Florez Paz, and Dr. Yoshichika Baba from the Department of Physiology & Cellular Biophysics, Columbia University, for providing insightful suggestions.

Competing financial interests

The authors declare no competing financial interests.

References:

Anandagoda N, Willis JC, Hertweck A, Roberts LB, Jackson I, Gokmen MR, Jenner RG, Howard JK, Lord GM. MicroRNA-142-mediated repression of phosphodiesterase 3B critically regulates peripheral immune tolerance. J. Clin. Invest. 2019;129:1257–1271.

Chiu IM, von Hehn CA, Woolf CJ. Neurogenic inflammation and the peripheral nervous system in host defense and immunopathology. Nat. Neurosci 2012;15:1063–1067.

Colucci V, Strichartz G, Jolesz F, Vykhodtseva N, Hynynen K. Focused ultrasound effects on nerve action potential in vitro. Ultrasound Med. Biol 2009;35:1737–1747.

Cotero V, Fan Y, Tsaava T, Kressel A M, Hancu I, Fitzgerald P, Wallace, K, Kaanumalle S, Graf J, Rigby W, Kao TZ, Roberts J, Bhushan C, Joel S, Coleman TR, Zanos S, Tracey KJ, Ashe

J, Chavan SS, Puleo C. Non-invasive sub-organ ultrasound stimulation for targeted neuromodulation. Nat Commun 2019;10:952.

Downs ME, Lee SA, Yang G, Kim S, Wang Q, Konofagou EE. Non-invasive peripheral nerve stimulation via focused ultrasound in vivo. Phys Med Biol 2018;63:035011.

Foley JL, Little JW, Staar FL, Frantz C, Vaezy S. Image-guided HIFU neurolysis of peripheral nerves to treat spasticity and pain. Ultrasound Med. Biol 2004;30:1199–1207.

Foley JL, Little JW, Vaezy S. Image-guided high-intensity focused ultrasound for conduction block of peripheral nerves. Ann Biomed Eng 2007;35:109–119.

Foley JL, Little JW, Vaezy S. Effects of high-intensity focused ultrasound on nerve conduction. Muscle Nerve 2008;37:241–250.

Fontaine AK, Anderson HE, Caldwell JH, Weir RF. Optical readout and modulation of peripheral nerve activity. Neural Regen. Res 2018;13:58.

George MS, Aston-Jones G. Non-invasive techniques for probing neurocircuitry and treating illness: vagus nerve stimulation (VNS), transcranial magnetic stimulation (TMS) and transcranial direct current stimulation (tDCS). Neuropsychopharmacology 2010;35:301–316.

Hovaguimian A, Gibbons CH. Diagnosis and treatment of pain in small-fiber neuropathy. Current pain and headache reports 2011;15:193–200.

Jancsó N, Jancsó-Gábor A, Szolcsányi J. Direct evidence for neurogenic inflammation and its prevention by denervation and pretreatment with capsaicin. Br. J. Pharmacol 1967;31:138–151.

Jancsó N, Jancsó-Gábor A, Szolcsányi J. The role of sensory nerve endings in neurogenic inflammation induced in human skin and in the eye and paw of the rat. Br. J. Pharmacol 1968; 33;32–41.

Kamimura HAS, Lee SA, Niimi Y, Aurup C, Kim MG, Konofagou EE. Focused ultrasound stimulation of median nerve modulates somatosensory evoked responses 2019 IEEE International Ultrasonics Symposium (IUS) 1085–1087

Kamimura HAS, Aurup C, Bendau E, Saharkhiz N, Kim MG, Konofagou EE. Iterative curve fitting of the bioheat transfer equation for thermocouple-based temperature estimation in vitro and in vivo. IEEE Trans Ultrason Ferroelectr Freq Control 2020;67:70–80.

Kim MG, Kamimura HAS, Lee SA, Aurup C, Kwon N, Konofagou EE. Image-guided focused ultrasound modulates electrically evoked motor neuronal activity in the mouse peripheral nervous system in vivo. J Neural Eng 2020;17:026026.

Kramer HH, Schmelz M, Birklein F, Bickel A. Electrically stimulated axon reflexes are diminished in diabetic small fiber neuropathies. Diabetes 2004;53:769–774.

Lin Q, Wu J, Willis WD. Dorsal root reflexes and cutaneous neurogenic inflammation after intradermal injection of capsaicin in rats. J. Neurophysiol 1999;82:2602–2611.

Lin Q, Zou X, Fang L, Willis WD. Sympathetic modulation of acute cutaneous flare induced by intradermal injection of capsaicin in anesthetized rats. J. Neurophysiol 2003;89:853–861.

Magerl W, Szolscany J, Westerman RA, Handwerker HO. Laser doppler measurements of skin vasodilatation elicited by percutaneous electrical stimulation of nociceptors in humans. Neurosci Lett 1987;82:349–354.

Mihran RT, Barnes FS, Wachtel H. Temporally-specific modification of myelinated axon excitability in vitro following a single ultrasound pulse. Ultrasound Med Biol 1990;16:297–309.

Mikami N, Matsushita H, Kato T, Kawasaki R, Sawazaki T, Kishimoto T, Ogitani Y, Watanabe K, Miyagi Y, Sueda K, Fukada SI, Yamamoto H, Tsujikawa K. Calcitonin gene-related peptide is an important regulator of cutaneous immunity: effect on dendritic cell and T cell functions. J Immunol 2011;186:6886–6893.

Moe JH, Post HW. Functional electrical stimulation for ambulation in hemiplegia J Lancet 1962;82:285–288.

Rochlitzer S, Veres TZ, Kuhne K, Prenzler F, Pilzner C, Knothe S, Winkler C, Lauenstein HD, Willart M, Hammad H, Muller M, Krug N, Lambrecht BN, Braun A. The neuropeptide calcitonin gene-related peptide affects allergic airway inflammation by modulating dendritic cell function. Clin Exp Allergy 2011;41:1609–1621.

Sauerstein K, Klede M, Hilliges M, Schmelz M. Electrically evoked neuropeptide release and neurogenic inflammation differ between rat and human skin. J. Physiol. 2000;529:803-810.

Sheffler LR, Chae J. Neuromuscular electrical stimulation in neurorehabilitation Muscle Nerve 2007;35: 562–590.

Sluka KA, Willis WD, Westlund KN. The role of dorsal root reflexes in neurogenic inflammation. Pain Forum 1995;4:141–149.

Skaper SD, Facci L, Zusso M, Giusti P. An inflammation-centric view of neurological disease: beyond the neuron. Front. Cell. Neurosci 2018;12:72.

Talbot S, Abdulnour RE, Burkett PR, Lee S, Cronin SJ, Pascal MA, Laedermann C, Foster SL, Tran JV, Lai N, Chiu IM, Ghasemlou N, Dibiase M, Roberson D, Hehn CV, Agac B, Haworth O, Seki H, Penninger JM, Kuchroo VK, Bean BP, Levy BD, Woolf CJ. Silencing nociceptor neurons reduces allergic airway inflammation. Neuron 2015; 87:341–54.

Tsui PH, Wang SH, Huang CC. In vitro effects of ultrasound with different energies on the conduction properties of neural tissue. Ultrasonics 2005;437:560–565.

Weber M, Birklein F, Neundorfer B, Schmelz M. Facilitated neurogenic inflammation in complex regional pain syndrome. Pain 2001;91:251–257.

Weidner C, Schmelz M, Schmidt R, Hansson B, Handwerker HO, Torebjörk HE. Functional attributes discriminating mechano-insensitive and mechano-responsive C nociceptors in human skin. Journal of Neuroscience 1999;19:10184–10190.

Wright CJ, Haqshenas SR, Rothwell J, Saffari N. Unmyelinated peripheral nerves can be stimulated in vitro using pulsed ultrasound. Ultrasound Med. Biol 2017;44:2269–83.

Young RR, Henneman E. Reversible block of nerve conduction by ultrasound. Arch Neurol 1961;4:83–89.

Zachs DP, Offutt SJ, Graham RS, Kim Y, Mueller J, Auger JL, Schuldt NJ, Kaiser CRW, Heiler AP, Dutta R, Guo H, Alford JK, Binstadt BA, Lim HH. Non-invasive ultrasound stimulation of the spleen to treat inflammatory arthritis. Nat Commun 2019;10:951.

Zhi MJ, Liu K, Zheng ZL, He X, Li T, Sun G, Zhang M, Wang FC, Gao XY, Zhu B. Application of the chronic constriction injury of the partial sciatic nerve model to assess acupuncture analgesia. J. Pain Res 2017;10:2271–2280.

Figure Captions

Figure 1. The experimental setup is composed of (a) an image-guided FUS stimulation system, a 3D positioning system, a high-resolution laser Doppler imaging, and a blood flow recording and analysis equipment. After finding the targeted distal sciatic nerve based on both ultrasound B-mode imaging and muscle activation conducted by image-guided FUS, the effects of FUS were recorded by time-based blood flow change monitoring at the plantar view of the hind paw. (b) Results of analysis of the effect of FUS in terms of response latency, time-to-peak, peak increase in blood flow, and area under the curve and normalized to baseline values before FUS.

Figure 2. Time-based blood flow measurement following (a) experimental groups applying FUS to the sciatic nerve (n=8) and negative control groups either deactivating the FUS driving system (n=7) or applying 20 dB attenuated FUS with a center frequency of 3.1 Hz and PRF of 0.1 Hz (n=6) with the rest of the experimental setup kept the same.

A distinct blood flow pattern induced by FUS was observed compared to the negative control experiments. (b) The time-to-peak value from FUS stimulation was not significantly different from the two negative control groups' values. (c) FUS induced a rapid increase in the blood flow change, which caused a decrease in the response latency compared to the negative control groups. (d) FUS led to a significant increase of area under the curve, which remained at a higher level during and after FUS stimulation. (e) The FUS-mediated peak increase in blood flow was significantly higher than those in the negative control groups.

Figure 3. Time-resolved blood flow change mediated by (a) on-target FUS at the sciatic nerve (n=8) or off-target FUS at 2.5 mm from the nerve region (n=6). A distinct blood flow pattern was observed after FUS stimulation at the sciatic nerve. (b) Following FUS on the nerve region, time-to-peak significantly exceeded that following FUS at 2.5 mm away from the focus. (c) Both FUS stimulation at on-target and off-target contributed to a rapid increase in the response latency (d) on-target FUS led to a significant increase in area under the curve compared to off-target FUS. (e) The blood flow presented a higher peak increase for on-target FUS versus off-target FUS, but there was no significant difference between them.

Figure 4. Time courses of blood flow change following (a) FUS of 10 min (n=8) and 3 min (n=2), electrical stimulation with subthreshold intensity (n=2). Similar blood flow patterns were observed between FUS of 10 min and 3 min. (b, c) No significant differences in time-to-peak or response latency were determined between FUS of 10 min and FUS of 3 min

with electrical stimulation with subthreshold intensity. (d, e) Electrical stimulation with subthreshold intensity did not evoke a significant increase in area under the curve or a peak increase in blood flow. However, FUS of 3 min increased blood flow in terms of area under the curve and peak increase in blood flow, which was not significantly different from the values from FUS of 10 min.

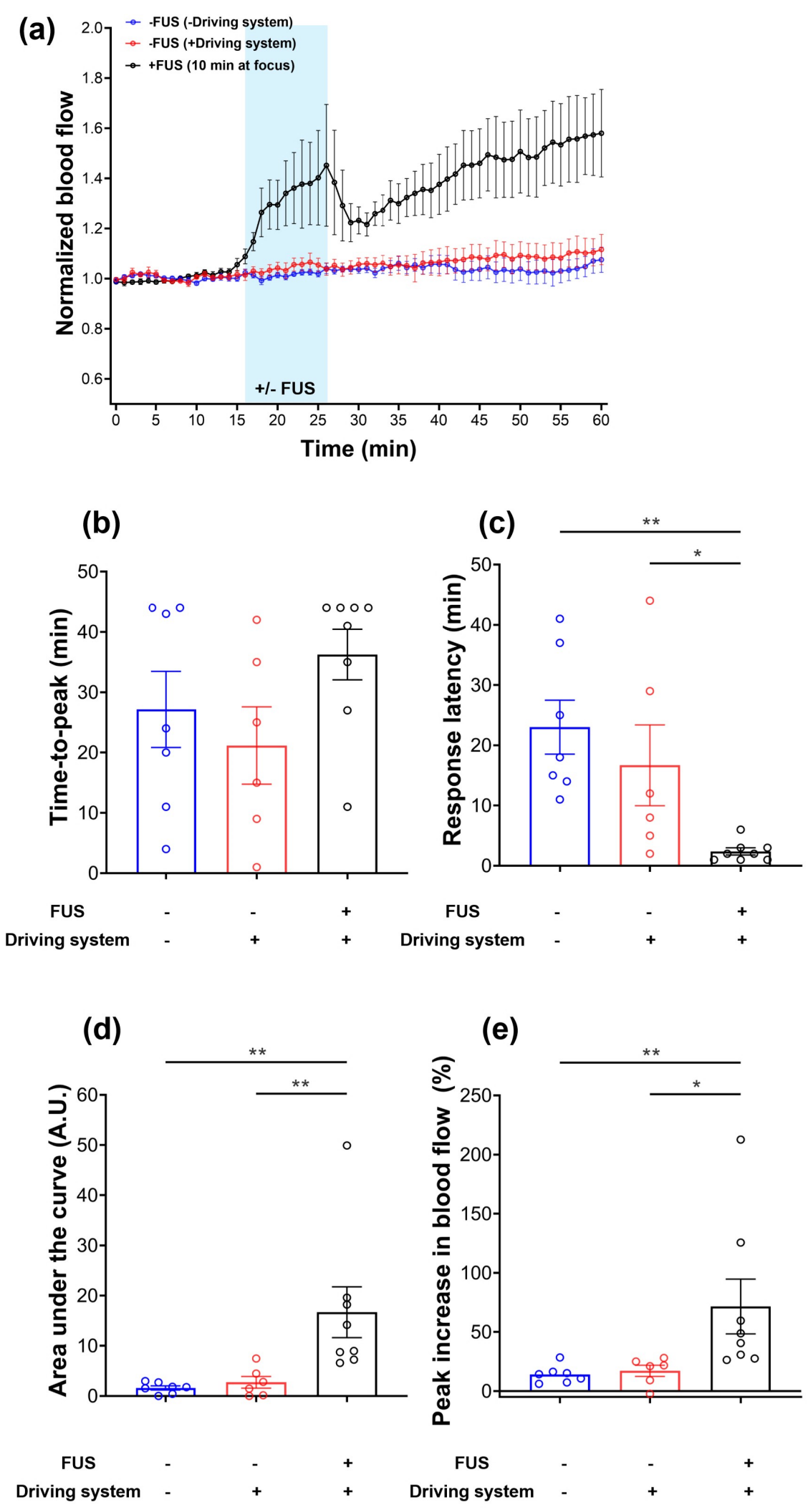
(a)
-FUS (-Driving system)
-FUS (+Driving system)
+FUS (10 min at focus)
Normalized blood flow
+/- FUS
Time (min)
(b)
Time-to-peak (min)
FUS
Driving system
(c)
Response latency (min)
**
*
FUS
Driving system
(d)
Area under the curve (A.U.)
**
**
FUS
Driving system
(e)
Peak increase in blood flow (%)
**
*
FUS
Driving system

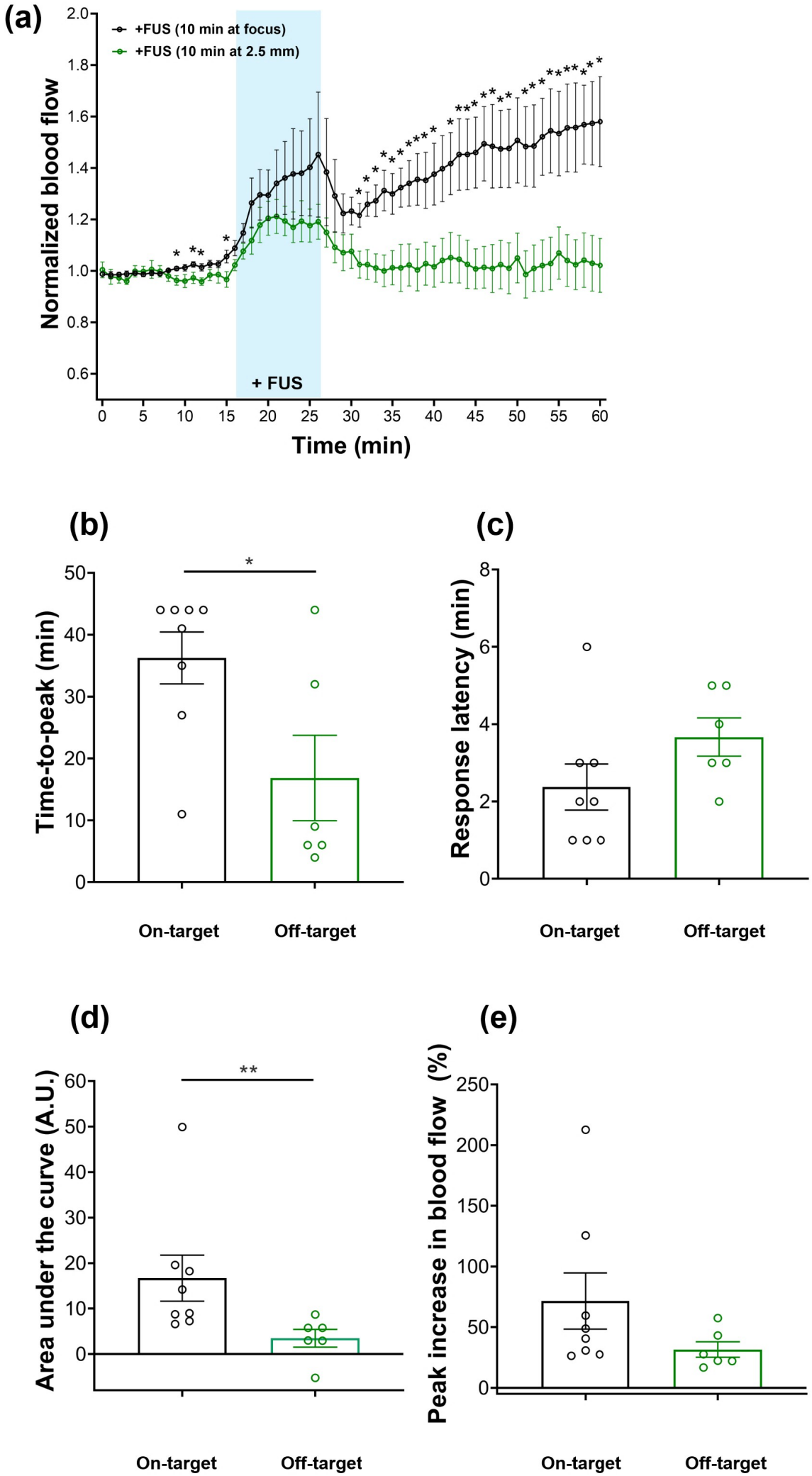
(a)
+FUS (10 min at focus)
+FUS (10 min at 2.5 mm)
Normalized blood flow
+ FUS
Time (min)
(b)
Time-to-peak (min)
On-target
Off-target
(c)
Response latency (min)
On-target
Off-target
(d)
Area under the curve (A.U.)
On-target
Off-target
(e)
Peak increase in blood flow (%)
On-target
Off-target

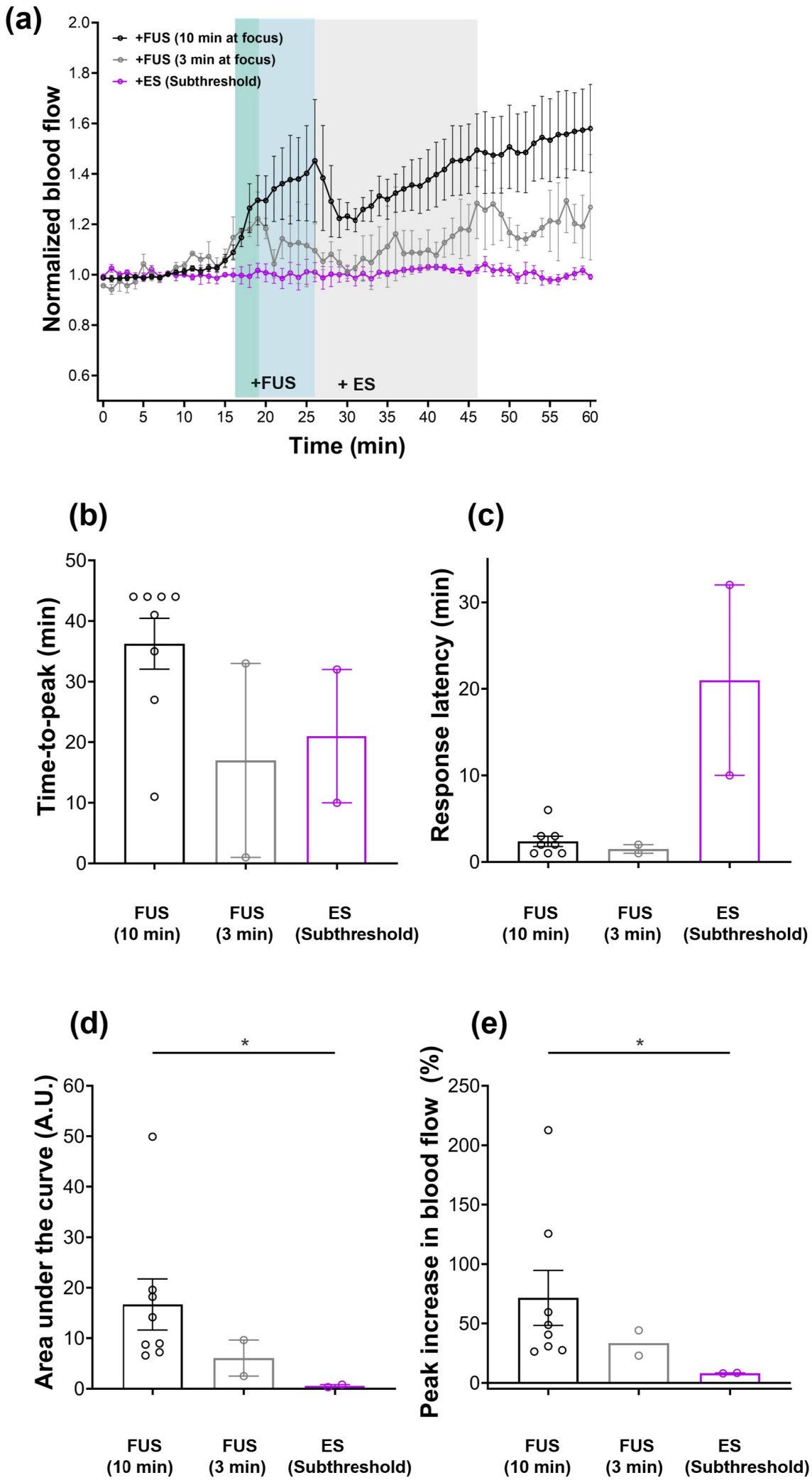
(a)
+FUS (10 min at focus)
+FUS (3 min at focus)
+ES (Subthreshold)
Normalized blood flow
+FUS
+ ES
Time (min)
(b)
Time-to-peak (min)
FUS (10 min)
FUS (3 min)
ES (Subthreshold)
(c)
Response latency (min)
FUS (10 min)
FUS (3 min)
ES (Subthreshold)
(d)
*
Area under the curve (A.U.)
FUS (10 min)
FUS (3 min)
ES (Subthreshold)
(e)
*
Peak increase in blood flow (%)
FUS (10 min)
FUS (3 min)
ES (Subthreshold)

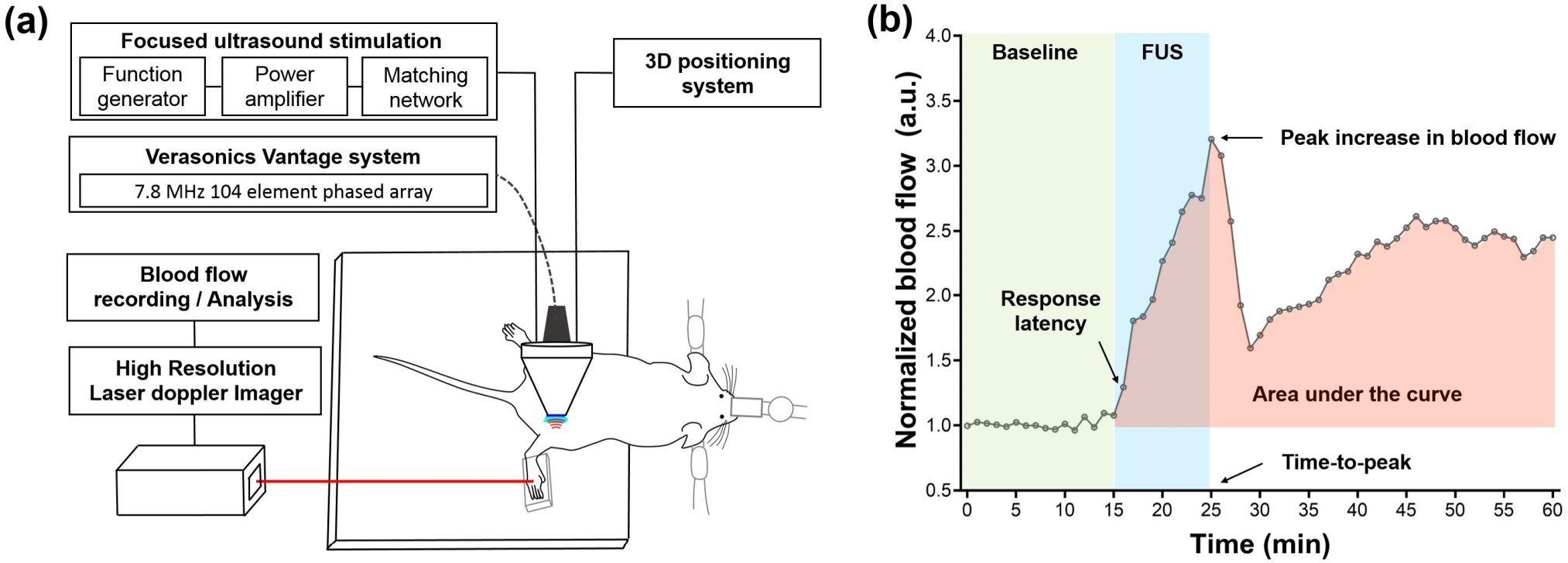
(a)
Focused ultrasound stimulation
Function generator
Power amplifier
Matching network
3D positioning system
Verasonics Vantage system
7.8 MHz 104 element phased array
Blood flow recording / Analysis
High Resolution Laser doppler Imager
(b)
Baseline
FUS
Peak increase in blood flow
Response latency
Area under the curve
Time-to-peak
Normalized blood flow (a.u.)
Time (min)
4.0
3.5
3.0
2.5
2.0
1.5
1.0
0.5
0
5
10
15
20
25
30
35
40
45
50
55
60